J Petrol Explor Prod Technol (2016) 6:617–628
DOI 10.1007/s13202-016-0236-8

ORIGINAL PAPER - PRODUCTION GEOPHYSICS

An inversion of reservoir properties based on a concurrent modeling approach: the case of a West African reservoir

Mukhtar Habib[1] · Samba Prisca Charles[2] · Yao Guangqing[1] · Musa Salihu Danlami[1] · Xie Congjiao[1] · Hamza Jakada[3] · H. A. Abba[4,5] · Ibrahim Abdullateef Omeiza[3]

Received: 20 May 2015 / Accepted: 9 February 2016 / Published online: 9 March 2016

Abstract Deterministic rock physics models were applied in a shale-sand environment located in the West African lower Congo basin, with the aim of estimating total porosity and clay content from P-wave acoustic impedance. Assuming that the only minerals within the target reservoir are quartz and clay, Han et al. model was used to determine the clay content which is referred herein as model-based *C*, while Krief et al. model was applied to solve the P-wave impedance for total porosity and clay content. The latter operation is a challenging task because of the nature of the actual rock physics equation that relates the known acoustic impedance to three unknown reservoir properties. This inherent difficulty is circumvented by making use of an additional linear equation, which is derived from the petrophysical link between porosity and clay content. To achieve this goal, firstly, a rock physics model was established, and then the reservoir was delineated through a combination of P-wave impedance and Poisson's ratio. In the reservoir, total porosity and clay content were inverted based on P-wave impedance by applying the rock physics model of Krief et al. that related P-wave impedance to total porosity and clay content, alongside the established petrophysical link between the two reservoir properties. The result was found to be consistent on the well log scale. Uniquely, a good match was obtained when the methodology was repeated on the real seismic data.

Keywords Porosity · Clay content · Model based clay content · Petrophysical link · Rock physics

✉ Yao Guangqing
gqyao@cug.edu.cn

[1] Faculty of Earth Resources, Key Laboratory of Tectonics and Petroleum Resources, China University of Geosciences, Wuhan 430074, Hubei, China

[2] Petroleum Exploration and Production Research Institute of Sinopec, Beijing, China

[3] School of Environmental Studies, China University of Geosciences, Wuhan 430074, Hubei, China

[4] Department of Geology, China University of Geosciences, Wuhan 430074, Hubei, China

[5] MAUTECH, Yola, Adamawa, Nigeria

Introduction

The estimation of petrophysical parameters (total Porosity ϕ and clay content C) is very important in terms of model building, volumetric reserve estimation as well as overall field development planning. However, obtaining reservoir properties from seismic inversion data is not trivial because most of seismic models do not take into account the poroelasticity. There is a plethora of studies in literature aiming at converting bandlimited seismic data into reservoir properties. Considering previous works, Maureau and Van Wijhe (1979) and Angeleri and Carpi (1982) inferred porosity using the linear link between inverted impedance and porosity log, Doyen et al. (1996) employed geostatistics techniques to get porosity maps, Batzle and Wang (1992) derived pore fluid parameters from seismic properties, Hampson and Russell (2005) used multi-attribute transform and neural network to predict porosity, Koesoemadinata and McMechan (2001) applied empirical rock physics relationship to derive reservoir parameters. Recently, some authors have shown the importance of deriving reservoir properties simultaneously. Bachrach (2006) and Sengupta and Bachrach (2007) succeed in simultaneously inverting both porosity and water saturation by using stochastic rock physics modeling. With reference to Sengupta and Bachrach (2007), but with an emphasis on

deterministic rock physics and petrophysical links, P-wave impedance was inverted herein for total porosity and clay content.

Various reservoir prediction models have been proposed by several authors, the common forward models utilized are on the basis of statistical analysis which work better when computing elastic properties if ϕ and C are known (Tosaya and Nur 1982; Castagna et al. 1985; Han et al. 1986; Eberhart-Phillips 1989; Marion and Jizba 1997). For this category of models, a noteworthy match between Han et al. (1986) model and the data utilized was observed during the rock physics diagnostic. Han et al. (1986) derived some equations that provide a significant contribution in finding other possible reasons for velocity reduction. The equations were derived by means of statistical methods using 75 different brine saturated sandstone samples with porosity ranging from 3 to 30 % and clay volume ranging from 0 to 55 %. These equations, which relate velocities (P and S-waves) to total porosity and clay content, revealed that sonic velocity gets reduced with an increase in the amount of clay volume. Another contribution is the possibility of obtaining elastic properties when the values of porosity, clay content and confining pressure are known. Inversely, clay content can be obtained if P-wave velocity, porosity and confining pressure are known.

The rock physics models of Raymer et al. (1980), Willie et al. (1956) and Krief et al. (1990), although established for single mineral (pure sand) and single fluid, are of great interest with regard to the inversion of reservoir properties since they can be adapted with fluid and lithology mixtures. For this category of models, Krief et al. (1990) model was preferred because of its ability to fit in describing the data utilized herein much better than others. Krief et al. (1990) derived a relationship between the squares of velocities (P and S-waves) and porosity. Having been developed specifically for one solid and one fluid, Krief et al. (1990) equations try to explain the influence of lithology and fluid content on velocities. In addition to Han et al. (1986) model which focuses only on the influence of clay content and porosity on sonic velocity, Krief et al. (1990) model takes also into account the fluid content effects. Krief et al. (1990) equations, although established for single mineral (pure sand) and single fluid, can be rewritten considering the Sand shale mixture, and even the fluid mixture. The fact that Krief et al. (1990) equations have been half theoretically derived coupled with their adaptation to different types of mixtures makes the equations relevant for inversion purposes.

Incorporating lithology and fluid mixtures in Krief's model, so as to estimate rock properties, is a challenging task, because of the nature of the derived rock physics equation. One known parameter, which is the P-wave acoustic impedance and three unknowns which are total porosity, clay content and water saturation (most often assumed), are considered herein. The possibilities of overcoming this difficulty can be achieved using additional equations to get a determined system of equations, thereby overcoming the challenge posed by such expressions. Some authors prefer adding rock physics equations that relate S-wave impedance to rock properties as in Goldberg and Gurevich (1998). But, far from this approach, the trend observed on C versus ϕ cross-plot can also be used. Dvorkin and Gutierrez (2002) and Thomas and Stieber (1975) have thoroughly studied the link between ϕ and C, in which they have shown that ϕ and C are related in some depositional settings. This case study, therefore, makes use of the petrophysical link between clay content and total porosity, which is often observed in a dispersed shale environment, in a move to estimate reservoir properties from elastic properties. Meanwhile an inversion of I_p and v for ϕ and C becomes faster. Such an inversion is conducted in this paper. The work is based on data derived from a geologically matured marine environment in which elastic properties are related to reservoir properties by the models of Han et al. (1986) and Krief et al. (1990).

To accomplish this work, firstly a rock physics diagnostic was performed, during which two rock physics models were found to be of best fit with the data (Han et al. 1986; Krief et al. 1990) models. Therefore, at a confining pressure of 20 MPA, Han et al. (1986) equation that relate P-wave impedance to clay content and porosity was used to estimate the clay content which is referred herein as model-based C. A petrophysical linear equation was then derived from a cross-plot of the model-based C versus total porosity.

The reservoir interval was identified by cross-plotting P-impedance versus Poisson's ratio. Within the reservoir portion, Krief et al. (1990) equation (for P-wave impedance), together with the petrophysical linear equation was further applied to resolve I_p for ϕ and C. The outputs of this transformation were found to be the same as the initial porosity log and the model-based C. Finally, the real acoustic impedance data were then inverted into ϕ and C at well location. When compared with original logs, the last two reservoir properties were successfully inverted despite the number of assumptions, the linear petrophysical link and the challenges posed by seismic data.

Materials and methods

Two reservoir petrophysical properties (ϕ and C) and two reservoir elastic properties (acoustic impedance, I_p, and poisson ratio, v) were the primary parameters considered herein, because understanding of ϕ and C is required for a shaly sand reservoir.

Table 1 Fluid mineral properties

	Bulk modulus (GPa)	Shear modulus (GPa)	Density (g/cm^3)
Brine	2.721	0	1.024
Oil	0.597	0	0.685
Quartz	36.6	45	2.65
Clay	21	7	2.58

Total porosity log is not neutral in the proposed methodology since it must be computed from density log, according to Eq. (1). The equation is based on the assumption that density of the mineral phase is fixed as 2.65 g/cm^3 while bulk density is based on brine saturated conditions.

$$\phi = \frac{2.65 - \rho_b}{2.65 - \rho_w} \tag{1}$$

$$\rho_b = (1 - \phi)\rho_s + \phi\rho_f \tag{2}$$

where ρ_b is the bulk density, ρ_w is the density of brine given in Table 1. ρ_s and ρ_f are densities of mineral and fluid phase, respectively.

Rock physics models

The proposed methodology aims at resolving ϕ and C from I_p by combining Han et al. (1986) with Krief et al. (1990) models; however, their applicability to the well log data has to be validated firstly.

Han et al. (1986) model

Han's model is a strong tool and a simple means of manipulating porosity and lithology as well as elastic wave velocity. The models were generated from a huge set of well log and core data, which provides relative degree of certainty that the models are efficient and can be utilized on other sets of data whose original backgrounds are analogous. Other simple empirical equations applicable for similar case are that of Willie et al. (1956) and Raymer et al. (1980).

Considering a confining pressure of 20 MPa, with velocities in km/s and sandstone samples are water charged, Han's equations applied herein are written as follows:

$$V_P = 5.49 - 6.94\phi - 2.17C \tag{3}$$

$$V_s = 3.39 - 4.73\phi - 1.81C \tag{4}$$

where V_p and V_s are compressional and shear wave velocities, respectively.

I_p and v as functions of V_p, V_s, and ρ_b are expressed in Eqs. (5) and (6), as follows;

$$I_p = \rho_b V_p \tag{5}$$

$$v = \frac{1}{2}\frac{V_p^2/V_s^2 - 2}{V_p^2/V_s^2 - 1} \tag{6}$$

The idea of using this model is to get C from initial V_p and V_s logs by applying the model-based approach. Hence, any of Eqs. (3) or (4) can be applied to get C which is define herein as model-based C.

As mentioned earlier, Han's equations were obtained for a particular saturating fluid (water). In other words, Han's model does not take into account other fluids, such as oil and/or gas. Therefore, the model cannot be readily used to invert P-impedance data for rock and fluid properties. Hence Krief et al. (1990) model was introduced to overcome this shortcoming.

Krief et al. (1990) model

It is worth stating that (Krief et al. 1990) velocity–porosity model was originally developed for one solid and one fluid. According to the model, acoustic impedance can be expressed as;

$$I_p = \sqrt{\left[\rho_s V_{ps}^2 (1 - \phi)^{\frac{3}{1-\phi}} + \beta^2 \times M\right] \times \rho_b} \tag{7}$$

Eq. (7) can be extended to the sand shale mixture as,

$$I_P = \sqrt{(\text{coef}\rho_s + (1 - \text{coef})\rho_f) \times \left\{\rho_s V_{ps}^2 \text{coef}^{\frac{3}{\text{coef}}} + \left[1 - (\text{coef})^{\frac{3}{\text{coef}}}\right]^2 \times \frac{K_s K_f}{\text{coef}(K_f - K_s) + K_s}\right\}} \tag{8}$$

$$\text{coef} = 1 - \phi \tag{9}$$

where ρ_b is the bulk density, ρ_f and K_f are the density and bulk modulus of the pore filling fluid, respectively, K_s, V_{ps} and ρ_s are the bulk modulus, P-wave velocity and density of the grain mineral, respectively. More details on Eq. (8) can be found in the appendix.

Krief's compressional and shear velocities which are used to compute the poisson ratio (v) from equation Eq. (6) were obtained by dividing Eqs. (8) and (14) by the bulk density (18).

To calculate I_p from Eq. (8), total porosity, water saturation and clay content are required. The model-based clay content (C) was preferred over the clay content derived from linearly scaled gamma ray. It was therefore used in Eq. (8), along with total porosity and the assumed water saturation. The choice of model-based C is explained by the fact that it is linked to elastic properties (V_p and V_s) through rock physics model of Han et al. (1986).

The fluid and mineral parameters ($K_{Quartz}, K_{Clay}, \rho_f, K_f, \rho_{clay}, \rho_{Quartz}$) are defined in Table 1. It is important to mention that these parameters can also be computed if the reservoir pressure, temperature and the salinity of the fluid are well known. Some authors prefer to predict them using consistent rock physics models.

Inversion

An established link (Eq. 11) between ϕ and C is incorporated into Eq. (8), to constrain the inversion. This gives a starting point for resolving I_p in respect of ϕ, by comparison of the original and modeled I_p (Eq. 8). Through iteration, porosity values are updated until an optimum porosity is achieved. Then it is straightforward to estimate C from Eq. (11), by utilizing the optimum porosity in Eq. (8).

Figure 1 shows the workflow of the methodology used for inverting both ϕ and C from I_p. It starts from (1) well log quality control (QC) and conditioning to ensure that the required data were available and physically reasonable in support of petrophysics and rock physics activities, (2) petrophysical analysis is conducted on processed and conditioned well logs for the generation of important petrophysical log curves, such as ϕ and C; (3) based on conditioned logs (measured V_p, V_s and ρ), elastic properties such as I_p and v are computed and fluid substitution is performed through Gassmann (1956) equations so as to bring all data to 100 % brine. Then a rock physics diagnostics is performed by cross-plotting I_p and v versus ϕ. The idea here is to select a model that matches the well log data. A model-based clay content is generated from the selected Han et al. (1986) model, while Krief et al. (1990) model is selected for resolving I_p. Shear and compressional velocities derived from Krief's model are used to compute v; (4) reservoir rock portion is delineated on the bases of I_p and v cross-plot color coded by porosity log; (5) a petrophysical link between ϕ and model-based C is established, while Krief's equation that relates P-wave impedance to total porosity and clay content is combined with the petrophysical link to resolve ϕ and C from I_p.

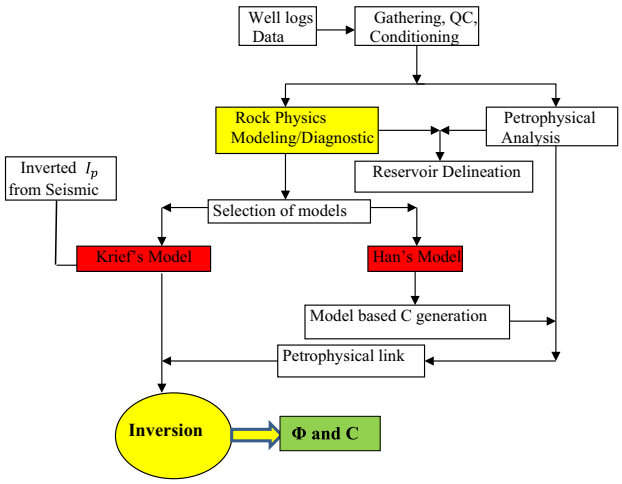

Fig. 1 Detailed workflow of the methodology

Results and discussion (case study)

This study is based on well log data derived from the West African Congo basin. A marine environment characterized by thick shale above a shaly/sand oil layer. The Miocene target reservoir is a series of turbidite sediments deposited on a broader valley; its upper part consists of homogeneous sandy deposits (Fig. 2 in interval 2912–2931 m), followed by prograding shaly deposits. The lower part is the turbidite deposit composed of sandy deposits with intercalated shaley layers (Fig. 2 in interval 2997–3098 m). After correcting initial well data (density, compressional and shear velocities logs, etc.) with spurious values by the help of rock physics modeling, petrophysical analysis, rock physics modeling and diagnostic were conducted.

Petrophysical analysis

Porosities of the reservoir sands range from 15 to 30 % and get reduced with an increased amount of clay content, thereby causing a velocity reduction Fig. 2. This observation was an important clue by assuming that the only minerals within the study area are quartz and clay.

A lithology indicator (GR log) was utilized to derive shale volume and clay content. This is done by linearly scaling GR to put forward a maximum and minimum C that corresponds to the GR, in which C values of 0.07 for minimum GR (pure sand) and 0.93 for maximum GR (pure shale) were assumed.

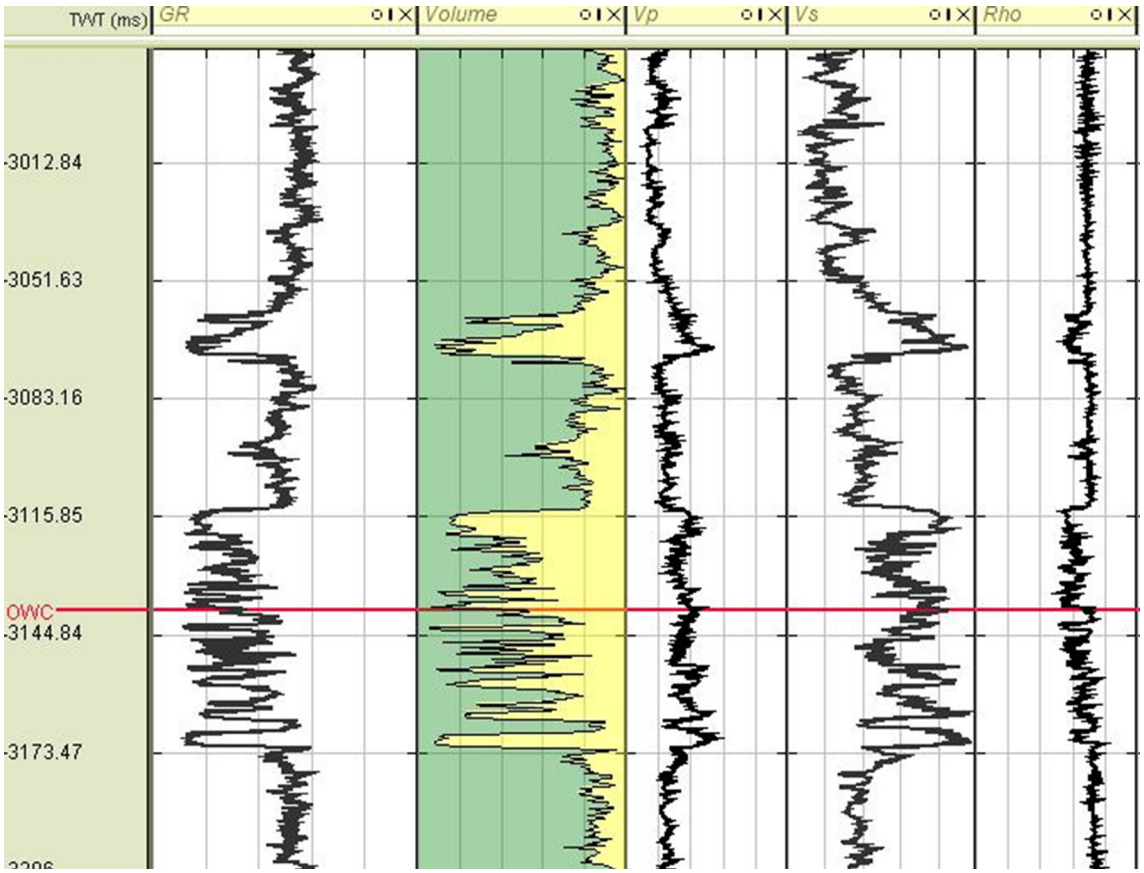

Fig. 2 Well log curve applied for this study. From *left* to *right* gamma ray, clay content, P-velocity, S-velocity and density

Rock physics modeling and diagnostics

This step comprises rock physics diagnostics which consist of trying several rock physics models to determine the one that best fit the data. Since majority of rock physics models were derived from brine saturated rocks, the actual original oil bearing reservoir was replaced by 100 % brine through Gassmann equations. Two models were found to explain and describe well the targeted well logs data:

Han et al. (1986) model

Han et al. (1986) model curves for I_p and v have been calculated for different values of C, which was found to match the data as depicted in Fig. 3 (left and right). On I_p or v versus total porosity cross-plot overlain by Han's model at different values of C, there is a noteworthy correspondence between Han's model and the data (Fig. 3). It is therefore clear that both ϕ and C significantly affected I_p. It can also be seen from Fig. 3 (left) that at a constant C, I_p increases with a decrease in ϕ. Conversely, at a constant ϕ, C decreases with an increase in I_p. This dependence property of V_p and I_p on C was carefully presented by Tosaya and Nur (1982); Castagna et al. (1985); Han et al. (1986). In Fig. 3 (right), value of v calculated at 100 % water saturation was presented, so as to serve the purpose of understanding the dependence of v on ϕ and C and/or lithology. It can be seen that both ϕ and C significantly affect v, it can also be observed that at a constant C, an increase in v corresponds to an increase in ϕ, while at a constant ϕ a large value of C also represents a large value of v. The dependence of v on ϕ is always clear in sand and shaly formations. It is apparent that this dependence is strongly linked to lithology because ϕ and lithology vary together. The yellow rectangle on Fig. 3 depicts the limits of the target reservoir which is also colored in yellow on the GR curve shown in the figure. A close look of this figure reveals a C range of 0–0.55 for reservoir sand and that of the overburden shale at 0.45–0.95.

Han's model was selected for this study because the model was derived from empirical data for brine saturated consolidated sediments. Above all, the rock physics diagnostics revealed that the model matches the data from the study area, meaning that it is consistent with the geological background of the study interval. This makes the model predictive beyond the data set used for matching. Other

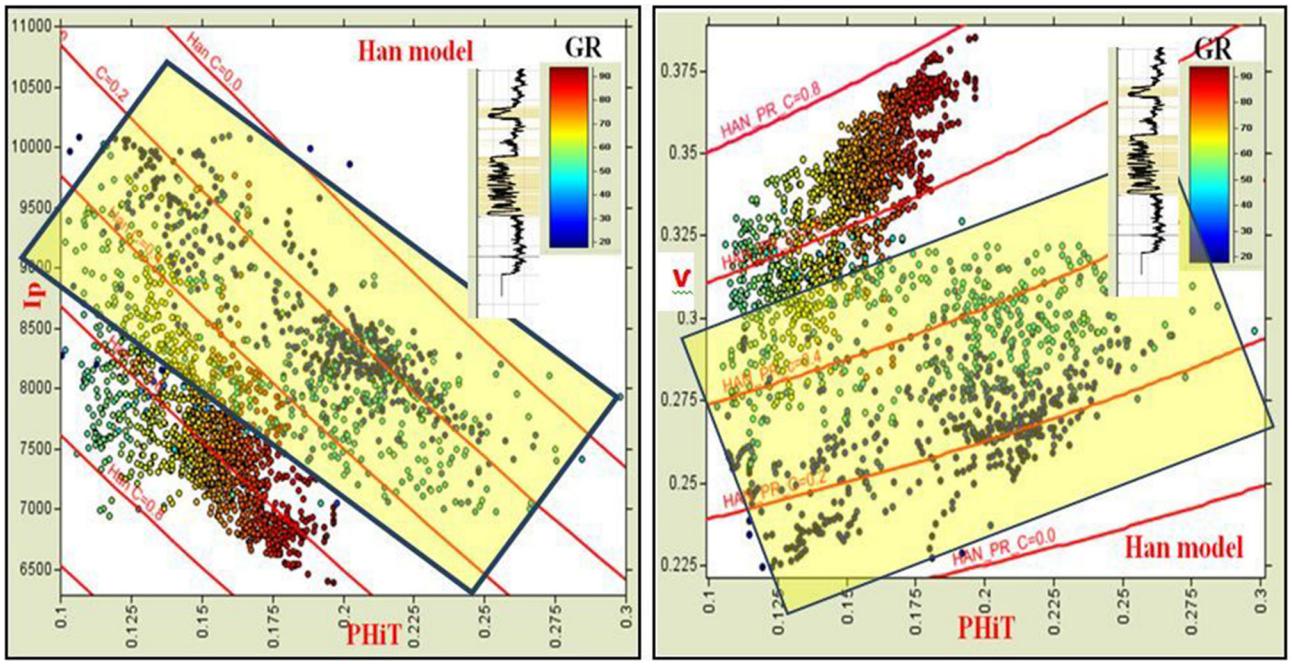

Fig. 3 Cross-plot of porosity versus P-impedance (*left*) and Poisson ratio (*right*) color coded by gamma ray. The overlain *red lines* are Han's models with different percentage of clay volumes

simple empirical equations applicable for similar case are that of Willie et al. (1956) and Raymer et al. (1980). But due to the fact that Han's model suitably describes and explains our data, it has been decided to apply it for getting the model-based clay content. Hence, any of Eqs. (3) or (4) was applied to get the model-based C.

The comparison between C derived from linearly scaled GR log (black) with the model-based C curve (red) is depicted in Fig. 4 (second panel), in which a similar trend is observed between the two. Meanwhile, the model-based C is used in the remaining part of this research.

Krief et al. (1990) model

Krief et al. (1990) model curves for I_p and v have been calculated for different values of C at 100 % water saturation, which was found to match the data as depicted in Fig. 5. This further revealed the applicability of the selected Krief's et al. model. The observed consistency between the model and the matching data is an important factor to be considered.

Krief et al. (1990) model was found to better describe and explain the real log data. Indeed, except some points, all the points representing the data fall nearly within the boundaries imposed by Krief model. In addition, it is clear that P-wave impedance gets reduced with an increase in the amount of clay volume, while the v decreases with a decreasing amount of clay volumes. This observation was also made by Han et al. (1986).

In the second frame of Fig. 6, the black curve comes from linearly scaled gamma ray curve while the red curve is the model-based C. On the other frames, the black logs are from the original curves whereas the red curves are calculated using Krief's et al. (1990) equations (Eq. (8) was applied for getting I_p, Eq. (8) divide by bulk density was applied for V_p and Eq. (14) divide by bulk density was applied for V_s). Hence, v was derived from compressional and shear velocities. The blue curves in the last two frames are the up-scaled logs. Figure 6 therefore shows a close match between the initial log curves and the developed curves (red), thereby proving the applicability of the selected models.

Reservoir delineation by combining I_p and v

The essence of this step is to make reservoir delineation so as to isolate the reservoir from the non-reservoir intervals by mapping two different domains (shale and sand). I_p and v logs computed during rock physics diagnostics as presented by Han et al. (1986) curves, together with existing ϕ log were used to delineate the sand reservoir from the non-reservoir shale. As presented by Fig. 3, the shale domain is having a C range of 0.45–0.95 which corresponds to a ϕ range of 0.1–0.125 presented by Fig. 7. Similarly, for the sand domain, a C range of 0.0–0.55 and a ϕ range of 0.125–0.22 was mapped. The pay sand and shale zones do not overlap, which means that the sand can be traced by seismic data through combining I_p and v. To make a clear

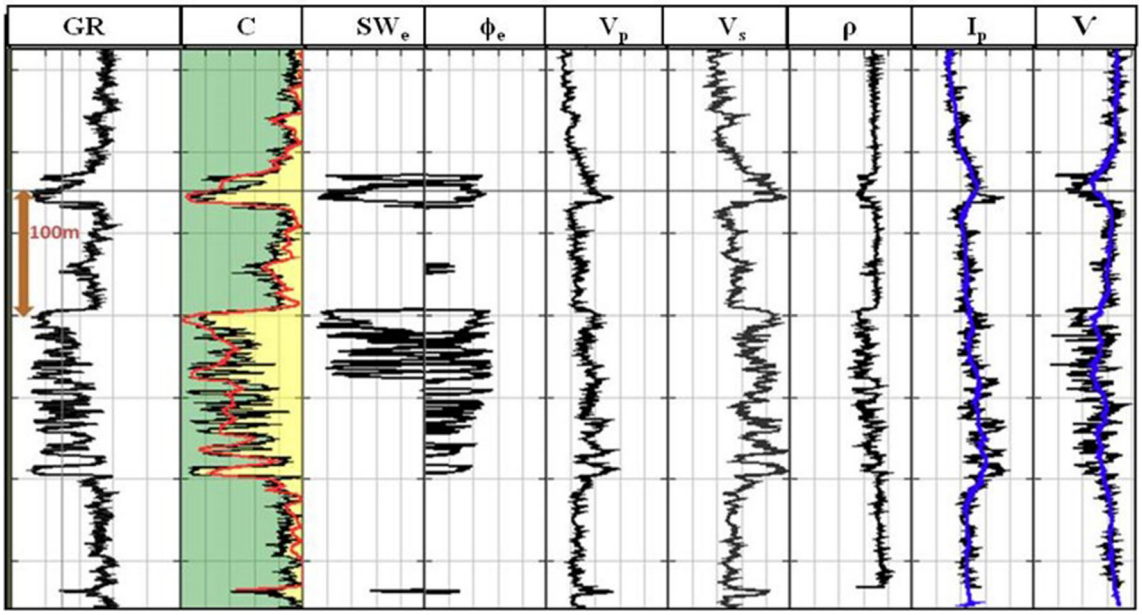

Fig. 4 Well log curve applied for this study. From *left* to *right* gamma ray, clay content, effective water saturation, effective porosity, P-velocity, S-velocity, density, P-impedance and Poisson's ratio. In the second frame, the *black curve* comes from linearly scaled gamma ray curve while the *red curve* is calculated as to match Han et al. (1986) model predictions

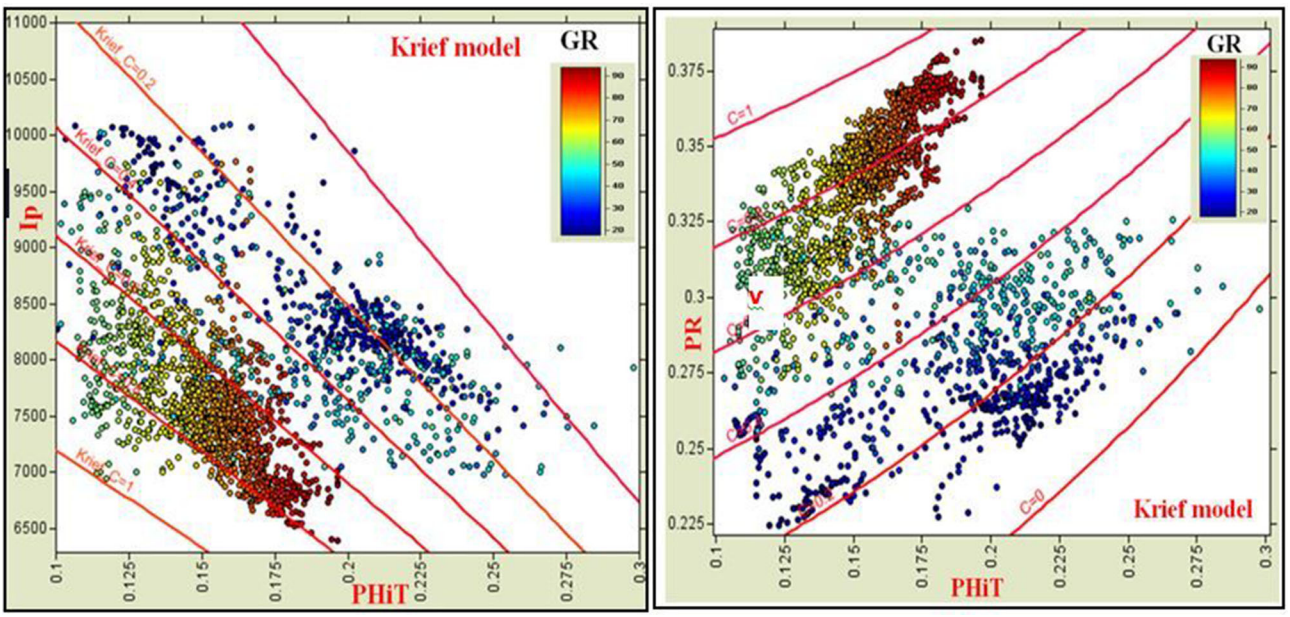

Fig. 5 Cross-plot of porosity versus P-impedance (*left*) and Poisson ratio (*right*) *color* coded by gamma ray. The overlain *red lines* are Krief et al. (1990) models with different percentage of clay volumes

demarcation, a cut-off line that would separate the shale zone from that of the sand was developed as shown in Fig. 7. Eventually, Eq. (10) was applied in respect of demarcation.

$$I_p = 35570.8v - 2661.4 \quad (10)$$

If $I_p < 35570.75v - 2661.45$, the zone is considered as sand and if $I_p \geq 35570.75v - 2661.45$, the zone is considered a shale zone. This cutoff value is apparently valid with log data. Is this cutoff value going to be the same on a seismic scale? To answer this question, a cross-plot of an up-scaled I_p and v logs was carried out, in which similar

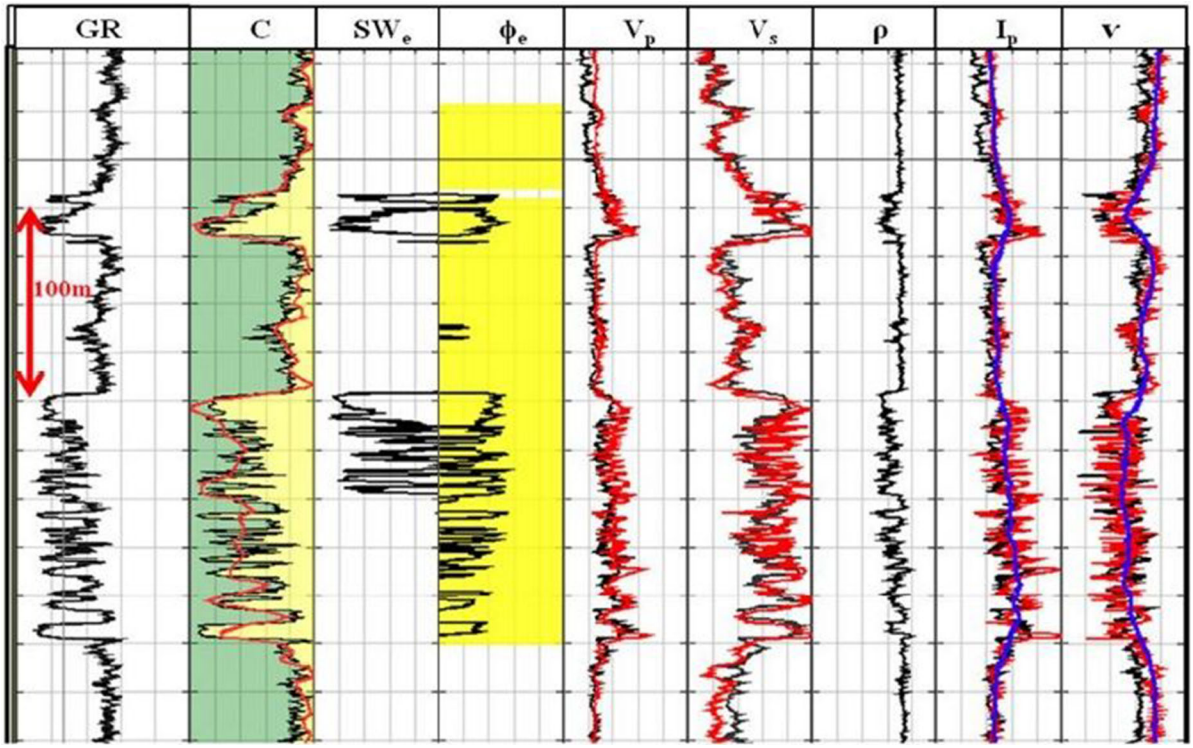

Fig. 6 Well log curve applied for this study. From *left* to *right* gamma ray, clay content, effective water saturation, effective porosity, P-velocity, S-velocity, density, P-wave impedance and Poisson's ratio

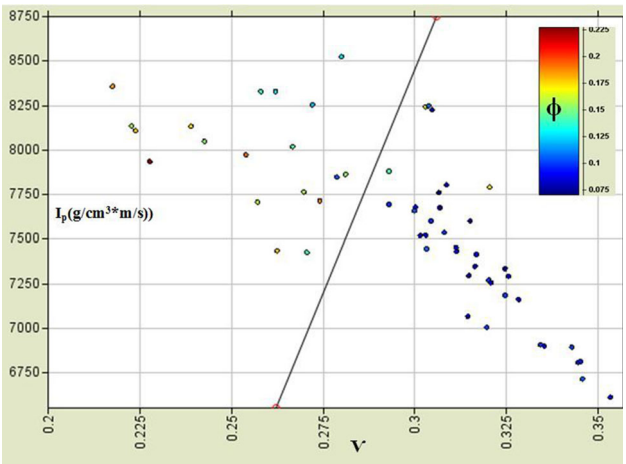

Fig. 7 Well log scale delineation. P-wave impedance versus Poisson's ratio *color* code by porosity, with sand and shale domains mapped in accordance with Eq. (10)

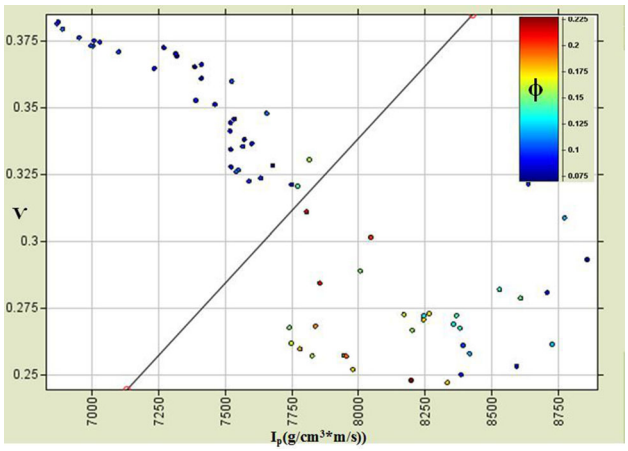

Fig. 8 Seismic scale delineation. P-wave impedance versus Poisson's ratio *color* code by porosity, with sand and shale domains separately mapped

trend with the well log scale model is observable. This has shown that the chosen cutoff value is valid for reservoir delineation (see Fig. 8).

Reservoir delineated at the seismic scale is slightly different from the actual one derived at the well log scale. This is because the up-scaled poison ratio curve has larger lower end values compared with the well log scale curve. This is a typical up-scaling artifact when converting to seismic from well log, therefore such a consideration has to be made while interpreting results.

It is therefore established that pay reservoir intervals can be detected from seismic data using a combination of seismically derived I_p and ν, as a result, inversion of I_p for ϕ and C in the sand can be attempted.

Petrophysical link between ϕ and C

With the aim of resolving the problem of underdetermined system of rock physics equations, the concept proposed by Thomas and Stieber (1975) was applied here to establish a desired link between ϕ and C so as to reduce the number of unknown reservoir properties. Considering one elastic property, the P-wave acoustic impedance (I_p) and three unknowns reservoir properties which are total porosity, clay content and water saturation (most often assumed).

Hence, the model-based C computed from Han's model and the ϕ derived from petrophysical analysis were applied. Figure 9 shows the cross-plot of ϕ versus the model-based C in which it can be observed that ϕ is relatively large but experiences a decrease as the value of C increases in the clean sand. This trend shows a turning point at $C = 0.5$, where the transition from sand to shale occurs thereby making a V-shaped pattern. This V-shape pattern is a characteristic of a bimodal sand/shaly mixture (Marion and Jizba 1997; Yin 1992).

Following the works of Dvorkin and Gutierrez (2002), the relationship between ϕ and model-based C was established using two linear equations. From the actual ϕ–C cross-plot, the trend within the sand reservoir is not well defined, while in the shale zone, the trend is quite clear. This observation revealed that for a shaly sand reservoir zone, several trends are possible. As a result, several trends in terms of linear equations were tested in the shaly sand zone. Thus, Eqs. (11) and (12) were found to be giving optimized results.

$$C < 0.5; \quad \phi = 0.188 - 0.0871C \tag{11}$$

$$C \geq 0.5; \quad \phi = 0.296 - 0.327C \tag{12}$$

Equation (11) which represents the reservoir portion will therefore be applied in the next section in order to constrain the reservoir inversion.

Inversion

Well log-based inversion

The established link between ϕ and C as described by Eq. (11) was then incorporated into Krief et al. (1990) model (Eq. 8). To compute I_p, the global elastic parameters portrayed in Table 1 were used, and the inversion result shown in Fig. 10 has depicted a match with initial reservoir measurements. The first column of this figure from left is the GR log in black, the second and third columns are ϕ and C volumes, respectively, with the initial measurement in black and inverted result in red. It is important to note that model-based C developed using Han et al. (1986) model has successfully been matched with the one generated by Krief et al. (1990) through inversion. This has proven a high degree of handshake between the two models.

Seismic-based inversion

At well location, the P-wave impedance obtained from inverting real seismic data was checked for consistency as

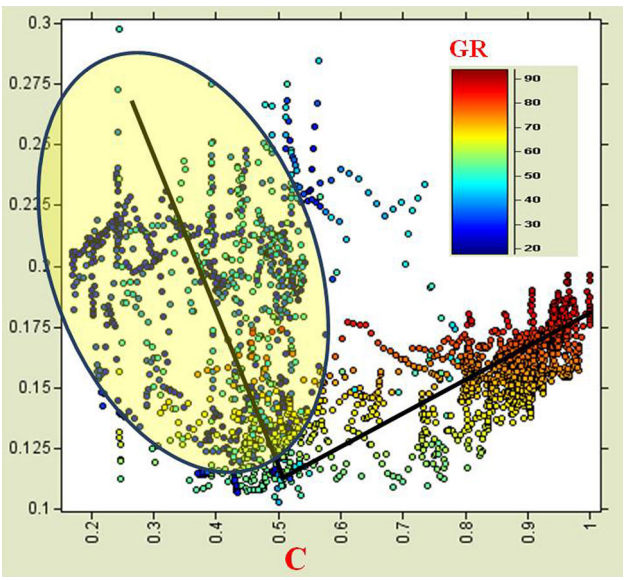

Fig. 9 Porosity as a function of clay content. *Straight lines* are in accordance with Eqs. (11) and (12). The *circled* part represents the reservoir

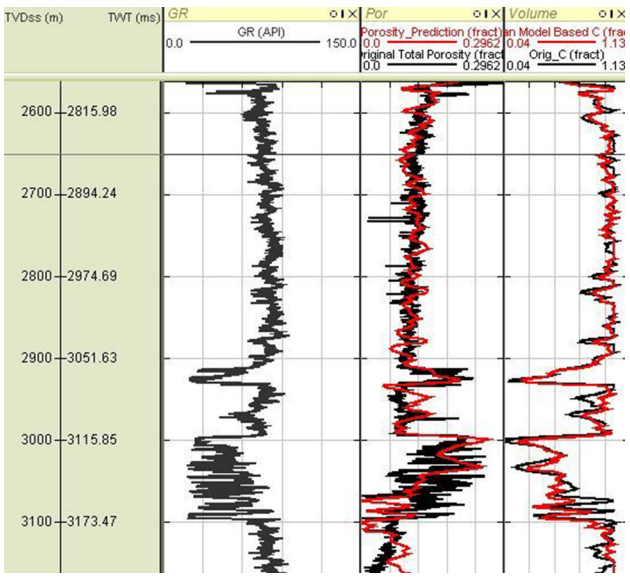

Fig. 10 Porosity and clay content predictions based on log scale acoustic impedance. From *left* to *right* (1) gamma ray; (2) the original porosity curve (*black*) and predicted porosity (*red*); (3) the original clay content (*black*) and predicted clay content (*red*)

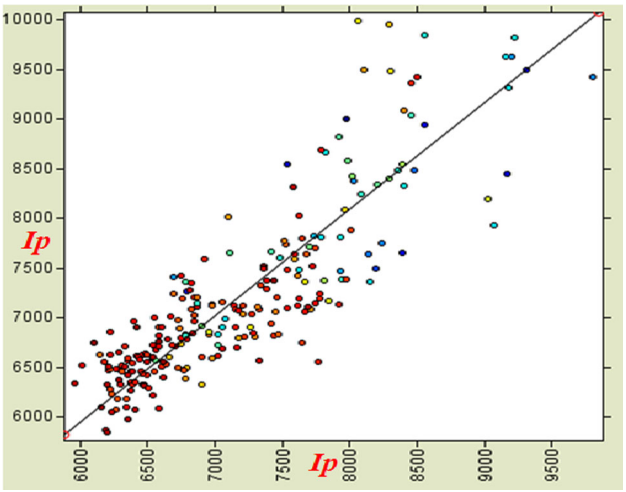

Fig. 11 Cross-plot of initial I_p in x axis versus inverted I_p in y axis. The unit of impedance is in g/cm^3 m/s

shown in the cross-plot of initial I_p in x axis versus inverted I_p in y axis (Fig. 11), where a good fit for impedances below 8000 g/cm^3 m/s was clearly observed. The proposed methodology was then applied to the real acoustic impedance, and the results were in good agreement with the previous tests (Fig. 12).

Conclusions

From this study a set of conclusions can be drawn:

1. Model-based C gives better results than a linear GR-based C when computing model-based Ip.
2. Both Han and Krief models explained the data pretty well. Han model was used to estimate the clay content which was referred to as model-based C. Krief model was employed to resolve the acoustic impedance for porosity and clay content.
3. Krief et al. model was applied for inversion based on the established (ϕ, C) link. An initial well log scale inversion has shown a very good match between the inverted C and the one derived from Han's model. This has proven a very clear conformity between the two models.

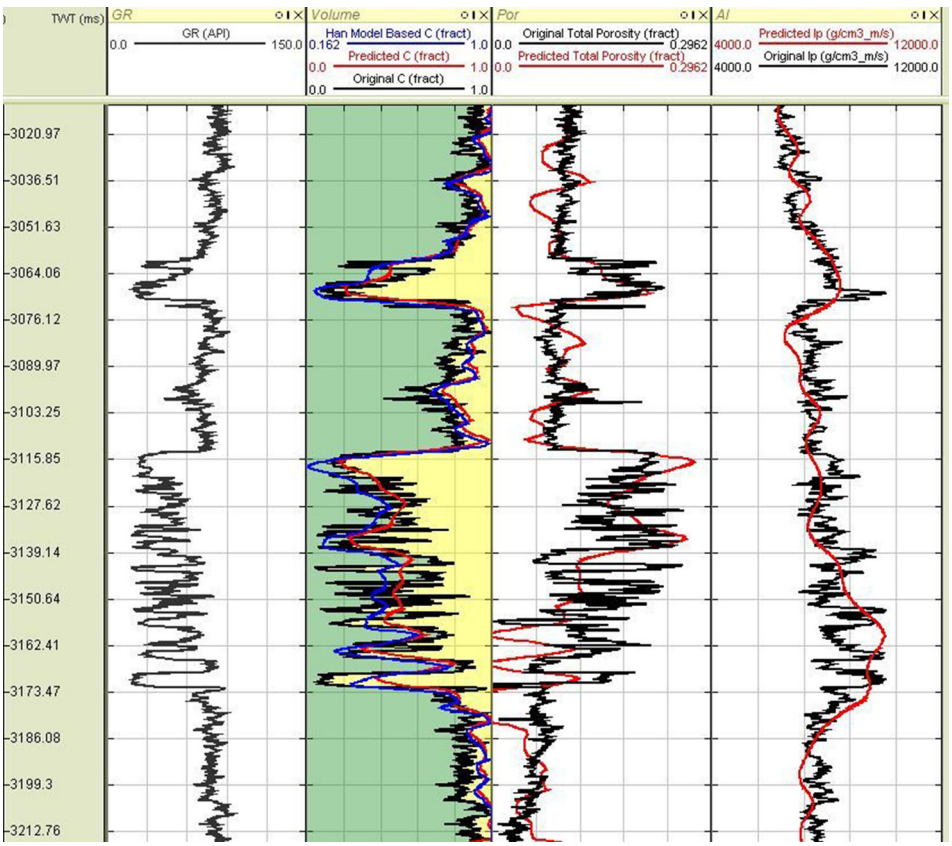

Fig. 12 Porosity and clay content predictions from real acoustic impedance. From *left* to *right*. (1) gamma ray; (2) the original (*black*) and predicted (*red*) clay content curves; (3) the original (*black*) and predicted (*red*) porosity curves; (4) the original (*black*) and predicted (*red*) acoustic impedance curves used for the inversion. In the *second panel*, *blue curve* is the model-based clay content derived from Han et al. (1986) model. A clear match between the original, inverted and model-based clay contents can be observed. In the *third panel*, a match between the original and the inverted total porosity is acceptable

4. At well location, the proposed methodology applied to real acoustic impedance data has shown encouraging results; therefore, it can be applied to the entire 3D survey which is going to be discussed in the next paper.
5. Models derived from such a methodology provide for reduced uncertainty in the sand/shale ratio, elastic moduli of pure minerals, mineral composition and the reservoir model itself. This will no doubt optimize the efficiency of reservoir performance and management.

$$\beta - \phi = (1-\phi) - (1-\phi)^{\frac{3}{1-\phi}} \tag{17}$$

The bulk density is written as follows;

$$\rho_b = \rho_s(1-\phi) + \rho_{fl}\phi \tag{18}$$

For sand shale mixture, using Hills average (Mavko et al. 1998), the bulk modulus of the grain mineral is given in Eq. (18);

$$K_s = \frac{(1-C)K_{quartz} + CK_{clay} + \frac{1}{\left[\frac{C}{K_{clay}} + \frac{(1-C)}{K_{quartz}}\right]}}{2} \tag{19}$$

$$\mu_s = \frac{(1-C)\mu_{quartz} + C\mu_{clay} + \frac{1}{\left[\frac{C}{\mu_{clay}} + \frac{(1-C)}{\mu_{quartz}}\right]}}{2} \tag{20}$$

Substituting Eqs. (15)–(19) into Eq. (13), one gets the acoustic impedance as a function of ϕ and C (Eq. 21).

$$I_P = \sqrt{(\text{coef}\rho_s + (1-\text{coef})\rho_f) \times \left\{\rho_s V_{ps}^2 \text{coef}^{\frac{3}{\text{coef}}} + \left[1 - (\text{coef})^{\frac{3}{\text{coef}}}\right]^2 \times \frac{K_s K_f}{\text{coef}(K_f - K_s) + K_s}\right\}} \tag{21}$$

Appendix

According to the Krief's model, acoustic impedance (I_p) and shear impedance (I_s) are written as follows,

$$I_p = \sqrt{\left[\rho_s V_s^2 (1-\phi)^{\frac{3}{1-\phi}} + \beta^2 M\right] \times \rho_b} \tag{13}$$

$$I_s = \sqrt{\rho_b \rho_s V_{ss}^2 (1-\phi)^{\frac{3}{(1-\phi)}}} \tag{14}$$

The pore space modulus M is computed using the theory of Gassmann as follows;

$$\frac{1}{M} = \frac{(\beta - \phi)}{K_s} + \frac{\phi}{K_{fl}} \tag{15}$$

After rearrangement the bulk compliance β coefficient is written as;

$$\beta^2 = \left[1 - (1-\phi)^{\frac{3}{1-\phi}}\right]^2 \tag{16}$$

Therefore, β can be written as;

where

$$\text{coef} = 1 - \phi \tag{22}$$

$V_{ps} = \sqrt{\frac{K_s + \frac{4}{3}\mu_s}{\rho_s}}$	P-wave velocity of the grain mineral (mixture)
$V_{ss} = \sqrt{\frac{\mu_s}{\rho_s}}$	S-wave velocity of the grain mineral (mixture)
$\rho_s = C\rho_{clay} + (1-C)\rho_{quartz}$	density of the grain mineral (mixture)

where ρ_f and K_f are the density and bulk modulus of the pore filling fluid, respectively, K_s, ρ_s, V_{ps}, V_{ss} are the bulk modulus, density, P-wave and shear wave velocities of the grain mineral.

References

Angeleri GP, Carpi R (1982) Porosity prediction from seismic data. Geophys Prospect 30:580–607

Bachrach R (2006) Joint estimation of porosity and saturation using stochastic rock-physics modeling. Geophysics 71(5):O53–O63

Batzle M, Wang Z (1992) Seismic properties of pore fluids. Geophysics 57(11):1396–1408. doi:10.1190/1.1443207

Castagna JP, Batzle ML, Eastwood RL (1985) Relationships between compressional-wave and shear-wave velocities in clastic silicate rocks. Geophysics 50(4):571–581. doi:10.1190/1.1441933

Doyen PM, Den Boer LD, Pillet WR (1996) Seismic porosity mapping in the Ekofisk field using a new form of collocated cokriging. SPE Annual Technical Conference and Exhibition, SPE 36498

Dvorkin J, Gutierrez MA (2002) Grain sorting, porosity and elasticity. Petrophysics 43:185–196

Eberhart-Phillips DM (1989) Investigation of crustal structure and active tectonic process in the cost ranges, central California. Ph.D. Dissertation, Standford University

Gassmann F (1956) Uber die Elastizitat Poroser Medien. Mitteilungen aus dem Institut fur Geophysik 17(96):1–23

Goldberg I, Gurevich B (1998) A semi-empirical velocity–porosity–clay model for petrophysical interpretation of P- and S-velocities. Geophys Prospect 46:271–285

Hampson DP, Russell BH (2005) Simultaneous inversion of pre-stack seismic data. 75th Annual International Meeting, SEG

Han D, Nur A, Morgan D(1986) Effects of porosity and clay content on wave velocity of sand stones. Geophysics 51:2093–2107

Koesoemadinata AP, McMechan GA (2001) Empirical estimation of viscoelastic seismic parameters from petrophysical properties of sandstones. Geophysics 66:1457–1470

Krief M, Garar J, Stellingwerff J, Ventre J (1990) A petrophysical interpretation using the velocities of P and S waves (full-waveform sonic). Log Anal 31:355–369

Marion D, Jizba D (1997) Acoustic properties of carbonate rocks: use in quantitative interpretation of sonic and seismic measurements. In: Palaz I, Marfurt KJ (eds) Carbonate Seismology. Society of Exploration Geophysicists, Tulsa, pp 75–94

Maureau G, Van Wijhe D (1979) The prediction of porosity in the Permian (Zechstein 2) carbonate of eastern Netherlands using seismic data. Geophysics 44:1502–1517

Mavko G, Mukerj T, Dvorkin J (eds) (1998) The rock physics hand book, tools for seismic analysis in porous media. Cambridge Press, Cambridge

Raymer DS, Hunt ER, Gardner JS (1980) An improved sonic transit time-to-porosity transform. Paper presented at the 21st annual meeting, society of petrophysist and well log analyst

Sengupta M, Bachrach R (2007) Uncertainty in seismic-based pay volume estimation: analysis using rock physics and Bayesian statistics. Lead Edge 26:184–189

Thomas EC, Stieber S (1975) The distribution of shale in sandstones and its effect upon porosity. SPWLA logging symposium transactions

Tosaya C, Nur A (1982) Effect of digenesis and clays on compressional velocities in rocks. Geophys Res Lett 21:41–70

Willie MRJ, Gregory AR, Gardner WL (1956) Elastic wave velocities in heterogenous porous media. Geophysics 21:41–70

Yin H (1992) Acoustic velocity and attenuation of rocks. Isotropy, intrinsic anisotropy, and stress induced anisotropy. Ph.D. thesis (unpublished), Stanford University